# Fermi-level pinning in an Al-Ge metal-semiconductor junction

S. Ciraci* and A. Baratoff
*IBM Research Division, Zurich Research Laboratory, 8803 Rüschlikon, Switzerland*

Inder P. Batra
*IBM Research Division, Almaden Research Center, 650 Harry Road, San Jose, California 95120-6099*
(Received 2 August 1990)

We studied the energetics and electronic structure of the lattice-matched Al-Ge heterostructure using the self-consistent-field pseudopotential method. We showed that interactions at the interface are on the atomic scale and lead to directional metal-semiconductor bonds subsequent to the elimination of dangling bonds by the adsorption of metal atoms. As previously established, these bonds elongate and become less localized upon metallization of the overlayer, but their directional character is shown to be maintained. Buckling of the metal layers at the interface is favored even though metal and semiconductor lattices are almost commensurate. An analysis of the state and charge density leads to the conclusion that the Fermi level is determined by the metal states that decay into the semiconductor. It is ruled out that the dangling-bond surface states (which become resonance states in the conduction-band continua of metal) determine the Fermi level for the Al-Ge heterostructure.

## I. INTRODUCTION

When a semiconductor is put in intimate contact with a metal, its bands become aligned so that they establish a common chemical potential. This usually leads to a shift of the semiconductor bands. Since the states with energies within the gap must decay into the semiconductor, the shift of the conduction-band edge and the resulting upward band bending in the case of $n$-type semiconductors forms a barrier (Schottky barrier or SB) for electrons incident from the metal. Thus, electrons with energies falling in the gap are prevented from entering into the semiconductor. Owing to the rectifying properties of metal-semiconductor contacts and the importance of achieving Ohmic contacts in semiconductor integrated circuits, this barrier has been a subject of continuing interest.[1] A great deal of effort has been devoted to the development of an understanding of metal-semiconductor ($M$-$S$) interfaces and SB formation on the microscopic level, starting from submonolayer up to thick metal coverage. Unfortunately, the accumulated experimental data indicate that several factors (such as coverage, interface structure, growth conditions, defects, etc.) influence the formation of SB. The important but not yet fully understood issue is how and where the Fermi level is pinned. In particular, the precise nature and origin of the electronic states responsible for the pinning have been the subject of much controversy. The current status of the subject and current theories have been reviewed extensively in Refs. 1–3.

According to the earliest mechanism proposed by Bardeen,[4] charge redistribution among high-density surface states in the band gap of the semiconductor fixes the barrier, which is therefore rather insensitive to the work function of the metal. Various Si surfaces covered by an alkali-metal atom monolayer seem to be the only $M$-$S$ systems found so far in which the Fermi level is determined by the dangling-bond surface states[5] present on such free surfaces. In such systems the weakly bound alkali-metal valence electrons are donated to empty surface-state bands in the bulk band gap of the semiconductor. Apart from this recent revival, Bardeen's model was abandoned on the grounds that surface states are usually eliminated from the gap owing to reconstruction and/or bond formation to metal atoms at the interface. Subsequently, the mechanism of pinning has been the subject of several theoretical methods. Heine[6] proposed that metal-induced gap states (MIGS), which propagate in the thick metal film but become evanescent in the semiconductor, are responsible for the pinning. Theories[7,8] derived from his idea, namely the concept of charge neutrality at the interface, have shown reasonable success in predicting SB heights of various $M$-$S$ junctions as well as band offsets in semiconductor heterostructures.

Representing the metal by jellium with the mean density of Al, Louie and Cohen[9] studied the electronic structure of a metal-Si junction within the repeated slab model. They thus neglected the lattice incommensurability between the Al and Si(111) surfaces and used boundary conditions to represent the wave functions in terms of plane waves. In fact, their self-consistent-field (SCF) pseudopotential calculations revealed states that are bulklike in the jellium and dangling-bond-like at the interface, but decay into Si. This was the first indication of MIGS based on a first-principles treatment of the electronic structure of a $M$-$S$ junction, although the atomic nature of the interface and thus the details of bond formation between Al-Si interface atoms were omitted. In fact, the effects of the $M$-$S$ interactions on the atomic scale, in particular the formation of $M$-$S$ bonds from the

 

semiconductor bonds, were clarified by the SCF calculations of Zhang *et al.*[10] Later, however, experiments led to a different conclusion, namely that the Fermi level can be pinned and thus the SB is formed even at submonolayer coverage.[11,12] As a result, different kinds of states, such as extrinsic defect states,[12] intrinsic surface states,[13] or adatom states,[14–16] have been postulated in order to determine the Fermi level.

Recently Lannoo[13] proposed that the SB heights and heterostructure band offsets can be related to the energy of dangling-bond surface states. In this proposal, the intrinsic states of the semiconductor become resonant states and, through conditions imposed by the Friedel sum rule expressing charge neutrality, their average energy aligns with the Fermi level of the deposited metal. Consequently the average energy of the dangling bonds is identified with Tersoff's[8] "midgap level."

To better understand the SB problem, we investigate the energetics and the electronic structure of the Al-Ge(001) junction at an atomistic level. In order to eliminate the sample-specific, growth-dependent, and highly diversified effects produced at incommensurate interfaces, we considered a nearly lattice matched *M-S* interface [Al on Ge(001)]. The detailed atomic structure of the interface, which was determined earlier by total-energy minimization,[17] was maintained to examine metal-semiconductor interactions on the atomic scale. The pinning mechanism for half-monolayer and monolayer metal coverage has been the subject of recent studies pointing out interesting coverage-dependent effects.[14,15] It was found that at half-monolayer coverage, chemisorption bonds and adatom Al states dominate the energy spectrum near the band gap and determine the Fermi level.[14] However, at the monolayer coverage (two Al atoms per surface Ge cell forming a uniform metal overlayer), metallic bonding sets in among the metal adatoms, leading to a (quasi-) two-dimensional metal characterized by a ladder-type density of states.[15] Concomitant with this metallization of the overlayer, the metal-semiconductor bonds are weakened (and slightly less localized) and the overlayer relaxes outwards away from the semiconductor surface. Even at this coverage the metal states with energies within the band gap cannot find matching partners and thus decay into the semiconductor. An important but not fully understood point is whether the delocalization of the *M-S* bond initiated by the metallization of the overlayer would increase with increasing overlayer thickness, so that the *M-S* bond would change into a resonant dangling bond. The interface atomic structure and in particular the transition from the diamond to the lattice-matched fcc structure is also of interest. Certainly, such effects can be studied by a detailed account of the atomic structure of the interface.

The present study also extends to earlier work[15–17] and treats a multilayer metal in contact with a covalent semiconductor. The entire arrangement is repeated periodically in three directions to form a superlattice. The prime issues we address are whether delocalization of bonds is complete at multilayer coverage and whether the resonant dangling bonds still remain and pin the Fermi level. We also address the role played by MIGS.

## II. DESCRIPTION OF CALCULATIONS AND ENERGETICS

Our results are extracted from standard SCF calculations with nonlocal ionic pseudopotentials[18] and a local exchange-correlation potential.[19] The Bloch states of the superlattice are expanded in terms of $\sim 1000$ plane waves corresponding to a kinetic-energy cutoff $|\mathbf{k}+\mathbf{G}|^2 \leq 10$ Ry. The total energy and atomic forces are calculated in the momentum representation[20] with a convergence criterion (rms deviation in potential energy) of $\sim 5\times 10^{-6}$ Ry. The atomic arrangement of the supercells used in the SCF calculations is illustrated in Fig. 1. The Al and Ge slabs each containing five layers, which are in contact and laterally lattice matched, are periodically repeated along the [001] direction. This is denoted as an $Al_{10}Ge_5$ superlattice. In the study of the individual electronic states we also performed calculations on the same *M-S* junction consisting of nine layers of Ge and seven layers of Al (which is denoted as an $Al_{14}Ge_9$ superlattice by using the same kinetic-energy cutoff). Pseudomorphic growth of an Al(001) film on a Ge(001) substrate has been achieved by molecular-beam epitaxy.[21] To achieve lattice matching, the Al(001) slab must be rotated 45° with respect to the ideal Ge(001) lattice.[21] In this case the lattice mismatch is only 1.2%, and can be accommodated for by the strain in the Al lattice.

Previous geometry minimizations carried out for one adsorbed Al atom per Ge(001) cell favored the bridge-site position, which provides a natural hybridization of Al-$sp^2$

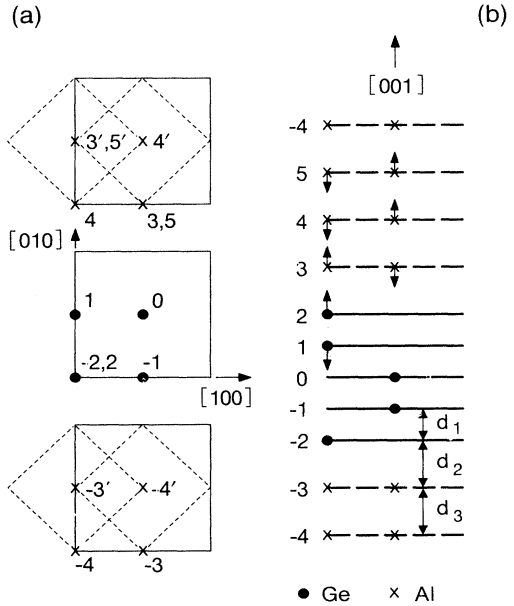


FIG. 1. Atomic arrangement in the $Al_{10}Ge_5$ supercell. (a) Top views from the [001] direction; inequivalent positions of metal atoms in the same layer are distinguished by primes. (b) Side view in the [010] direction; atomic planes are labeled by numerals. Arrows perpendicular to these planes indicate the directions and relative magnitudes of these forces given in Table I.

orbitals with the surface dangling bonds.[14,22] At this coverage (henceforth denoted as $\theta=1$), the Al atom was found adsorbed 2.3 a.u. above the top Ge layer with a binding energy of 3 eV. The maximum binding energy of the 45° rotated Al(001) layer [corresponding to two Al atoms per Ge(001) cell, or $\theta=2$], however, occurred at a significantly greater distance (3.4 a.u.), so that the directional Al—Ge bond was elongated but the bond charge was less localized.[14,15]

In the present calculations we started with $h=3.4$ a.u. for the Al-Ge interface spacing. For the Al-Al and Ge-Ge interlayer spacings in the sublattices, the optimum values determined for the bulk crystals are used and the metal layers are assumed to be planar. The perpendicular components of the forces acting on the atoms in the supercell are listed in Table I, and illustrated schematically in Fig. 1. Judging from Table I, neither the interlayer spacings nor the displacements of metal atoms in a given layer will be uniform. For example, while the Al atom at position 3 (see Fig. 1) will be lowered towards Ge, the second Al atom in the same plane but at position 3′ will also do so relative to the Ge plane but to a much lesser extent. This will result in a buckling of the metal planes. The degree of buckling, however, decreases farther away from the interface. In spite of these deformations, deviations from the structure described in Fig. 1 would not be significant enough to affect our conclusions regarding the Fermi-level pinning mechanism.

A comparison of the total energy of the superlattice with those of the Al and Ge lattices alone gives additional insight into the *M-S* interaction. To this end we calculated the total energy of the Al(Ge) slab by removing the Ge(Al) slab, thus keeping the same supercell and the kinetic-energy cutoff. The calculated values are $E_T[\mathrm{Al}]=-41.831$ Ry/cell and $E_T[\mathrm{Ge}]=-39.474$ Ry/cell. The total energy of an $Al_{10}Ge_5$ superlattice is calculated to be $-81.631$ Ry/cell. The adhesion energy of the metal overlayer per interface defined as

$$E_a=(E_T[\mathrm{Al}]+E_T[\mathrm{Ge}]-E_T[\mathrm{Al+Ge}])/2 \tag{1}$$

is therefore $E_a=2.24$ eV. The total energy is lowered owing to Al-Ge bond formation at the interface. However, the calculated value of $E_a$ is smaller than the binding energy of the single Al atom adsorbed at the bridge site. This reflects the weakening of the Al—Ge bond in the presence of the relatively stronger metallic bonding within the metal slab.

TABLE I. Perpendicular forces (along the $z$ direction) $F$, on atoms labeled in Fig. 1.

| Atom | $F$ ($10^{-9}$ N) |
|---|---|
| Ge(0) | ~0.0 |
| Ge(1) | −0.85 |
| Ge(2) | 1.15 |
| Al(3) | −0.27 |
| Al(3′) | 0.87 |
| Al(4) | −0.26 |
| Al(4′) | 0.15 |
| Al(5) | 0.10 |
| Al(5′) | −0.10 |

## III. ELECTRONIC STRUCTURE

We study the formation of *M-S* bonds by considering total and difference charge densities. The latter,

$$\Delta\rho(\mathbf{r})=\rho_{\mathrm{AlGe}}(\mathbf{r})-\rho_{\mathrm{Ge}}(\mathbf{r})-\rho_{\mathrm{Al}}(\mathbf{r}) \tag{2}$$

is obtained by subtracting the charge densities of free Al and Ge slabs from the charge density of an $Al_{10}Ge_5$ superlattice. The charge density of a free Al(Ge) slab is calculated by removing the Ge(Al) slab from the superstructure. In Fig. 2 we show contour plots of the charge densities $\rho_{\mathrm{Al}}(\mathbf{r})$, $\rho_{\mathrm{Ge}}(\mathbf{r})$, $\rho_{\mathrm{AlGe}}(\mathbf{r})$, and $\Delta\rho(\mathbf{r})$ calculated in the (100) and (010) planes. The $\Delta\rho$ plots show the formation of *M-S* bonds in both planes. The charge depleted from the upper lobes of the dangling bonds and from the adjacent Al is accumulated near the center of the Al—Ge bond. In the (100) plane, a *M-S* bond forms although the Al atoms in position 3′ do not continue the Ge—Ge bond sequence between adjacent layers (see Fig. 1). As expected the *M-S* bond is stronger in the (010) plane, in which Al in position 3 has the tetrahedral coordination. Comparing the bond in the (001) plane with that which forms at $\theta=1$ (i.e., for a single absorbed Al atom per Ge(001) unit cell at $h=2.3$ a.u.), we note that it becomes weaker in the presence of a thick metal overlayer. For example, $\rho_{\max}=0.079$ electrons/(a.u.)$^3$ along the bond at $\theta=1$, whereas the corresponding value in the present case is 0.058. We conclude that in the presence of a thick metal overlayer the *M-S* bonds in the interface become weaker and less localized, but the delocalization is not complete and thus the directional covalent character of the bonds is maintained.

The evolution of the electronic structure upon junction formation and the character of *M-S* bonds and other states with energies within or near the gap are analyzed by considering the total and interlayer densities of states, $D(E)$ and $L(E)$, respectively. The interlayer density of states between the layers $l_i$ and $l_{i+1}$ is defined as

$$L_{l_{i+1},l_i}(E)=\int_{l_i}^{l_{i+1}}\left[\sum_{n,k}\Psi^*_{n,k}(\mathbf{r})\Psi_{n,k}(\mathbf{r})\delta(E-E_{m,k})\right]d\mathbf{r}\ , \tag{3}$$

such that the integral $\int^{E_F}L_{i+1,l_i}(E)dE$ yields the amount of charge between the layers $l_i$ and $l_{i+1}$.

We calculated $D(E)$ and $L_{ij}(E)$ for 81 $k$ points uniformly distributed in the (001) plane passing through the $\Gamma$ point of the superlattice Brillouin zone. This sampling is rather crude but is expected to reveal basic features of the actual state densities upon broadening with a Gaussian of width comparable to the typical level spacing for fixed $\mathbf{k}$. Figure 3 shows total and interlayer densities calculated for the $Al_{10}Ge_5$ superlattice. The interlayer density of states is Ge-like between layers 0 and 1, but exhibits important metal-like and semiconductorlike features in the interface (i.e., between layers 2 and 3). On the metal side (between layers 3 and 4) it becomes metal-like. It

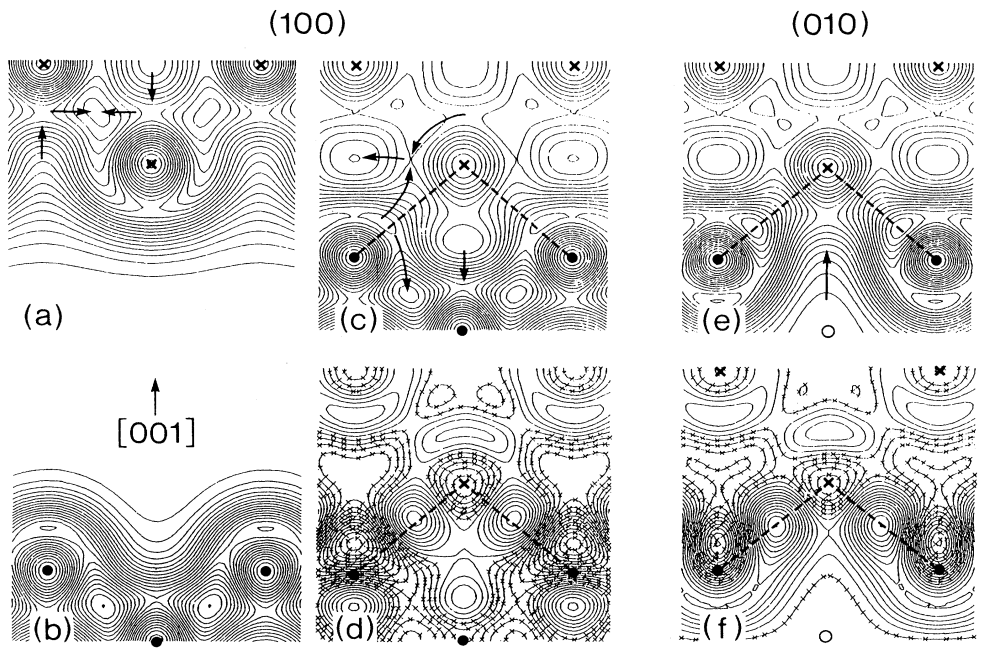


FIG. 2. Contour plots of total and difference (AlGe-Al-Ge) valence charge densities. (a) Al slab; (b) Ge slab; (c) $Al_{10}Ge_5$ superlattice with central Al at position 3′; (d) corresponding difference charge density; (e) $Al_{10}Ge_5$ superlattice with central Al at position 3; (f) corresponding difference charge density. Contour spacings are 15, 33, 33, 6.8, 27, and $8.2\times10^{-4}$ electrons/a.u.$^3$, respectively; arrows indicate directions of increasing density. Contours with crosses refer to negative values.

should be noted that $L_{0,1}$ has a finite density of states near $E_F$ (or in the gap). This is partly because some states leak down to the second layer of Ge, and is partly an artifact of the Gaussian broadening.

The total density of states of an $Al_{10}Ge_5$ superlattice is compared with those of the metal and semiconductor

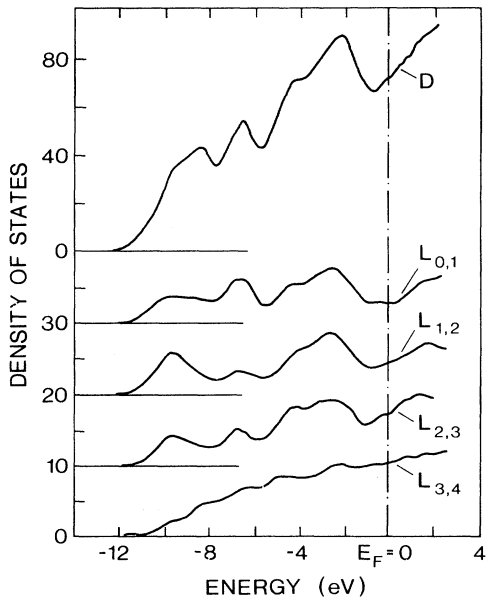


FIG. 3. Total ($D$) and interlayer ($L$) densities of states calculated for the Al-Ge superlattice. Subscripts indicate the layers specified in Fig. 1 between which the interlayer density of states has been calculated; thus $L_{2,3}$ denotes the Al-Ge interface.

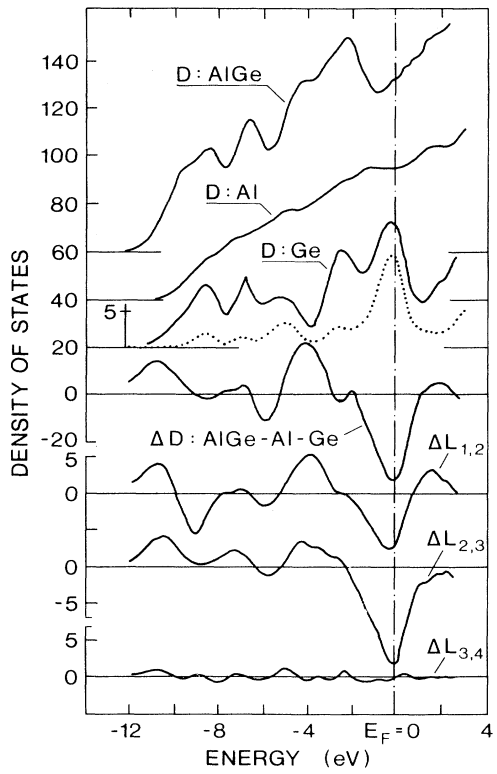


FIG. 4. Total ($D$) densities of states calculated for the $Al_{10}Ge_5$ superlattice, for the free Al and Ge slabs, and the surface contribution to the latter (dotted line with different scale), difference total density of states $\Delta D$ (AlGe-Al-Ge), and corresponding difference interlayer densities of states $\Delta L_{i,j}$, calculated between the layers $i$ and $j$.

slabs alone in Fig. 4. The contribution of the surface states (shown by dotted lines) to the density of states of the Ge slab is obtained by integrating from the surface Ge-layer to the vacuum. The surface contribution at $E_F$ originating from the intrinsic dangling-bond surface states exhibits a strong peak. The difference state density, i.e., $\Delta D = D^{\mathrm{AlGe}} - D^{\mathrm{Al}} - D^{\mathrm{Ge}}$ indicates that, upon junction formation, new states appear near $-4$ and $-11$ eV below $E_F$, whereas Ge-related features disappear near 0, $-6$, and $-9$ eV. The nature and origin of those changes are clarified by considering the difference interlayer densities of states, i.e., $\Delta L = L^{\mathrm{AlGe}} - L^{\mathrm{Al}} - L^{\mathrm{Ge}}$ calculated at the interface and in the adjacent regions above and below it. Dramatic changes occur at energies corresponding to *M-S* bonds ($-4$ and $-10$ eV) and those of dangling bonds and backbonds (from $-2$ eV to $E_F$) of the Ge slab. Intrinsic surface states of the free Ge slab are modified and shifted out of the band gap to form *M-S* bonds. No significant changes occur between the surface and subsurface layers of the Al sublattice. The amount of charge calculated between layers 2 and 3 (in the interface) is found to be approximately equal to the sum of those corresponding to the free Ge and free Al slabs calculated in the same region.

Additional insight into the rearrangement of the electronic states upon *M-S* junction formation is obtained by subtracting the state density of the Al sublattice from that of the $Al_{10}Ge_5$ superlattice. Since the dangling bonds of the Ge slab are eliminated, the remaining state density is similar to that of the bulk Ge, except for some structure below $E_F$, due to the *M-S* bond. In the interface, the corresponding interlayer density (i.e., $\Delta L_{2,3} = L_{2,3}^{\mathrm{AlGe}} - L_{2,3}^{\mathrm{Al}}$) is found to be negligible near $E_F$. This implies that the states of the Al-Ge junction near $E_F$ are essentially derived from the Al metal. However, $\Delta L_{1,2}$ has a finite density near $E_F$ for the reasons explained above.

To investigate the nature of states that determine the Fermi level of the junction, we next examine the charge distribution of the individual states of the Al-Ge superlattice. We keep in mind that for a lattice-matched junction the wave vector parallel to the interface is still a good quantum number. Propagating solutions at either site can be matched into one wave function if their energies and wave vectors coincide. Such a situation can easily take place in the junction with a simple metal such as Al, except for the states decaying into one side where they fall into a gap. For example, the lowest valence-band state of Ge is formed from the bonding combinations of 4*s* orbitals and occurs about 12 eV below the common Fermi level. Since the width of the conduction band of Al is only $\sim 11$ eV, the states of Ge having energies $-12 \leq E \leq -11$ decay into the metal. On the other hand, propagating metal states decay into the semiconductor if their energy falls in the gap of the semiconductor. The charge-density plots of two states calculated for a relatively large superlattice ($Al_{14}Ge_9$) and illustrated in Fig. 5 clarify these arguments. While the states at the bottom of the Ge valence band are Ge-like in the corresponding sublattice, their weight is close to zero in the metal. In contrast, the state at the Fermi level is metal-like, but decays into the semiconductor, and hence has almost zero weight beyond the second layer in the Ge sublattice.

The metal states at the Fermi level, but which fall in the thermal gap of semiconductor, are of particular interest. Previously, these states were designated metal-induced gap states and were found to be responsible for the pinning of the Fermi level. These states are expected to behave like intrinsic gap states (or dangling-bond states) of Ge near the interface. However, this does not mean that Ge dangling-bond states (which were eliminated upon adsorption of the metal monolayer) reappear at thick metal coverage but are concealed in the band continua of Al. The bond formation illustrated in Fig. 2 and the conclusions drawn from the difference density of states discussed in Figs. 3 and 4 also prompt us to reject the idea of reformation of dangling-bond states in the presence of thick metal coverage. The metal states will see the potential at the surface of the semiconductor, which is different not only from the reconstructed surface but also from the ideal surface. The dangling-bond states

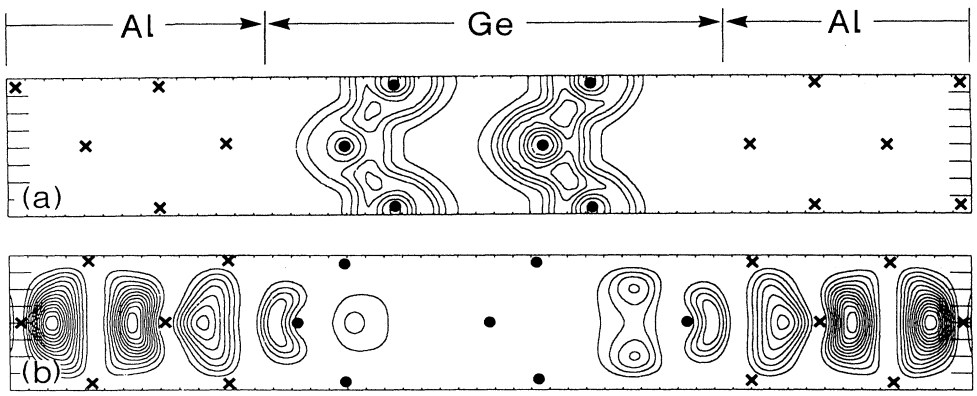


FIG. 5. Contour plots of the charge density of two typical states for $Al_{14}Ge_9$ superlattice shown in the corresponding supercell. (a) $E_\Gamma = -12.5$ eV; (b) $E_K = -0.07$ eV. Contour spacings are $10^{-4}$ electrons/(a.u.)$^3$, and energies of the states are given relative to the Fermi level. Al and Ge atoms are indicated by crosses and dots, respectively.

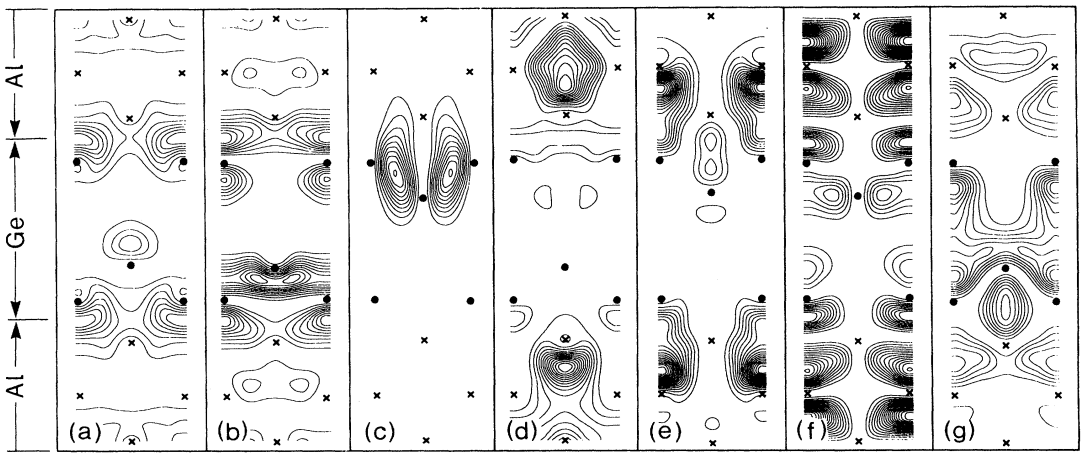


FIG. 6. Contour plots of the charge density of typical states for $Al_{10}Ge_5$ superlattice presented in the corresponding supercell. (a) $E_\Gamma = -9.78$ eV; (b) $E_\Gamma = -4.46$ eV; (c) $E_\Gamma = -3.13$ eV; (d) $E_\Gamma = -0.4$ eV; (e) $E_\Gamma \cong 0$ eV; (f) $E_K \cong 0$ eV; (g) $E_\Gamma = 0.6$ eV. Contour spacings are $10^{-4}$ electrons/(a.u.)$^3$, and energies of the states are given relative to the Fermi level.

would turn to the resonance states and broaden in energy near $E_F$ if the metal side were a jellium with its edge terminated between Al and Ge atomic planes at the interface. This is, however, an oversimplification omitting the *M-S* interactions on the atomic scale. The charge-density plots of the $Al_{10}Ge_5$ superlattice presented in Fig. 6 display the states that are relevant for the *M-S* junction.

The states in Figs. 6(a)–6(c) are associated with the Al—Ge bonds or the Ge—Ge backbonds near the interface. The state of Fig. 6(a) with $\sim -10$ eV relative to $E_F$ lies in the lowest peak in $\Delta D$ apparent in Fig. 3. It consists primarily of a bonding combination of Al and Ge orbitals. The state in Fig. 6(b) lies in the peak of $\Delta D$ at $\sim -4$ eV and is formed by Al $3p$ and Ge $4p_z$ orbitals. The state at $-3.2$ eV shown in Fig. 6(c) is also localized at the interface and corresponds to the backbonding state of Ge—Ge. The energies of the states in Fig. 6(c)–6(f) lie within the band gap of the Ge. They have a high density in the Al sublattice but decay into the Ge side. This behavior is characteristic of MIGS, which have almost zero weight 3–4 a.u. beyond the interface. However, as shown in Fig. 6(g), states that can match on both sides can propagate across both sublattices.

## IV. DISCUSSION

Based on the above results obtained for lattice-matched $Al_{10}Ge_5$ and $Al_{14}Ge_9$ we draw the following conclusions.

(i) Although Al is a simple metal that usually displays a nearly-free-electron-like behavior, its interaction with Ge at the interface is on the atomic scale. Directional bonds are formed between Al and Ge atoms at the interface as a result of a significant charge rearrangement relative to the free surfaces. The interface bonding energy is significant, but is smaller than the binding energy of the single adsorbed Al atom, and smaller than the cohesive energy per atom of Al metal as well. This is explained by the transfer of charge from the Al—Ge interface bonds to the Al overlayer upon the onset of overlayer metallization. Consequently, the weakened bonds are elongated and the metal overlayer is raised above the Ge surface. As shown earlier, this already occurs at the coverage of monolayer corresponding to a 2D metal.[14,15] Nevertheless, the *M-S* bonds are not completely delocalized as in the calculations[9] that represent the metal overlayer by a jellium, but maintain their directional character.

(ii) From analysis of the difference density of states, it is clear that the dangling-bond surface states are eliminated upon the junction formation, and form new *M-S* states in the valence band. No evidence was found that the surface dangling bonds are maintained as resonance although the weakening of *M-S* bonds at the interface does suggest such a possibility. Earlier calculations[9] yielded dangling-bond-like gap states at the interface. We suggest that this was the artifact of the model, which represented the metal overlayer by jellium with a sharp edge terminating halfway in the interface.

(iii) The states near $E_F$ have a high density in the metal film, but decay into the semiconductor. They have the character originally described by Heine,[6] and therefore are identified as metal-induced gap states. The formation of MIGS is reminiscent of confined states in semiconductor heterostructures. For example, because of the conduction-band offset, the band edge of one semiconductor sublattice in a GaAs-AlAs superlattice acts as a barrier for the conduction-band states of the adjacent sublattice that lies below this barrier.[23,24] Such states can therefore propagate in the first sublattice (quantum well) but must decay in the second one. If the width of the quantum well is small but the barrier is wide, one obtains 2D confined states.

The density of MIGS found in the present study is high enough to pin the Fermi level without invoking extrinsic states, such as defect or impurity states.[12] Of course, this conclusion does not rule out that the defect or impurity states can coexist with MIGS.

At this point it is in order to comment on the recent work by Das *et al.*[25] Using the linear-muffin-tin method within the local-density approximation, they carried out an extensive study of the epitactic $NiSi_2$-Si(111) interface

on the atomic scale. They found that the Fermi level is pinned by the interface states of semi-dangling-bond character. These states occur because of the reduced Si coordination of Ni at the interface. Bulk $NiSi_2$ is metal but has a partial gap for energies near $E_F$. In the NiSi-Si(111) junction this gap partially overlaps the band gap of Si, and the band of the interface states runs through the central part of the common gap. In compliance with our arguments in the preceding sections, the states, which fall into the common gap, decay at both sides and are localized at the interface. There should be, however, metal states at $E_F$, which fall into the band gap of Si and have the character of MIGS.

(iv) In his elaboration of Tersoff's theory,[8] Lannoo[13] identifies the charge neutrality midgap level with the dangling-bond energy $E_d$ at the free surface of the semiconductor. We note that $E_d$ is highly sensitive to surface structure and, in the case of some semiconductor surfaces, it can even dip into the band continua. Furthermore, the dangling-bond surface states required in the model proposed by Lannoo may not exist at all in some *M-S* systems. For example, consider a Ge(001) or Si(001) surface that is saturated by a monolayer of H prior to metal deposition. Although the energy gaps of these surfaces are then free of the intrinsic surface states, the Fermi level can still be pinned by MIGS. On the other hand, the dangling-bond surface states in the band gap can turn to resonance states (Breit-Wigner resonance) in the case of alkali-metal–semiconductor junction.[5,6] The charge neutrality midgap level is relevant because a dipole owing to the transfer of charge between metal and semiconductor (or between two semiconductors in a heterostructure) gives rise to a dramatic increase of energy, which cannot be balanced by the energy of bond formation. Therefore the electronic response to a certain interface structure in a *M-S* (or *S-S*) junction maintains the least amount of charge transfer to minimize the total energy. If the assumed junction geometry leads to a significant charge transfer and thus a rise of the total energy, the interface atomic structure can even be forced to reconstruct in order to lower the total energy. A typical example is the Ge-GaAs(001) interface.[26] These two semiconductors are nearly lattice matched so that GaAs may be thought to grow as a natural continuation of the Ge lattice. However, such an ideal junction nevertheless requires charge transfer at the interface, resulting in a metallic system, in which the Fermi level overlaps with the tilted valence-band continua. The dramatic increase in total energy has an electrostatic origin and is almost 1 order of magnitude higher for $Ge_4/(GaAs)_2$ than the formation energy of strained $Si_4/Ge_4$. This increase of the formation energy of the junction forces an atomic reconstruction at the interface. Therefore, the most fundamental criterion that fixes the position of the Fermi level is the minimization of total energy.[27] The charge neutrality concept is then a natural consequence of the former only in the majority of cases.

## ACKNOWLEDGMENTS

This work was partially supported by the Joint Project Agreement between Bilkent University and IBM Zurich Research Laboratory. The authors wish to thank E. P. Stoll for his valuable assistance.

*Permanent address: Department of Physics, Bilkent University, Bilkent 06533, Ankara, Turkey.

[1] *Metallization and Metal-Semiconductor Interfaces,* edited by I. P. Batra (Plenum, New York, 1989).
[2] R. H. Williams, Contemp. Phys. **23**, 329 (1982).
[3] L. J. Brillson, Surf. Sci. Rep. **2**, 123 (1982).
[4] J. Bardeen, Phys. Rev. **71**, 717 (1947).
[5] S. Ciraci and I. P. Batra, Phys. Rev. Lett. **56**, 877 (1986); Phys. Rev. B **37**, 2995 (1988); I. P. Batra and S. Ciraci, *ibid.* **39**, 3919 (1989).
[6] V. Heine, Phys. Rev. **138**, A1689 (1965).
[7] E. Louis, F. Yndurain, and F. Flores, Phys. Rev. B **13**, 4408 (1976).
[8] J. Tersoff, Phys. Rev. Lett. **52**, 465 (1984).
[9] S. G. Louie and M. L. Cohen, Phys. Rev. B **13**, 2461 (1976).
[10] S. B. Zhang, M. L. Cohen, and S. G. Louie, Phys. Rev. B **34**, 768 (1986).
[11] G. Margaritondo, J. E. Rowe, and S. B. Christman, Phys. Rev. B **14**, 5396 (1976).
[12] W. E. Spicer, I. Lindau, P. Skeath, C. Y. Su, and P. Chye, Phys. Rev. Lett. **44**, 420 (1980).
[13] M. Lannoo, Ref. 1, p. 259; I. Lefebrve, M. Lannoo, C. Priester, G. Allan, and C. Delerue, Phys. Rev. B **36**, 1336 (1987).
[14] I. P. Batra and S. Ciraci, Phys. Rev. B **29**, 6419 (1984); J. Vac. Sci. Technol. B **3**, 427 (1984).
[15] I. P. Batra and S. Ciraci, Phys. Rev. B **33**, 4312 (1986).
[16] W. Mönsh, Phys. Rev. Lett. **58**, 1260 (1987); Phys. Rev. B **37**, 7129 (1988); Ref. 1, p. 11.
[17] I. P. Batra, Phys. Rev. B **29**, 7108 (1984).
[18] D. R. Hamann, M. Schlüter, and C. Chiang, Phys. Rev. Lett. **43**, 1494 (1979).
[19] D. M. Ceperley and B. J. Alder, Phys. Rev. Lett. **45**, 566 (1980).
[20] J. Ihm, A. Zunger, and M. L. Cohen, J. Phys. C **12**, 4409 (1979); M. T. Yin and M. L. Cohen, Phys. Rev. B **26**, 3259 (1982); I. P. Batra, S. Ciraci, G. P. Srivastava, J. S. Nelson, and C. Y. Fong, *ibid.* **34**, 8246 (1986).
[21] Shang-Lin Weng, A. Y. Cho, W. C. Marra, and P. Eisenberger, Solid State Commun. **34**, 843 (1980).
[22] I. P. Batra, J. Vac. Sci. Technol. B **1**, 558 (1983).
[23] S. Ciraci and I. P. Batra, Phys. Rev. B **36**, 1225 (1987); **38**, 1835 (1988).
[24] E. Tekman and S. Ciraci, Phys. Rev. B **39**, 8772 (1989).
[25] G. P. Das, P. Blöchl, O. K. Andersen, N. E. Christensen, and O. Gunnarson, Phys. Rev. Lett. **63**, 1168 (1989).
[26] I. P. Batra, S. Ciraci, and E. Ozbay (unpublished).
[27] C. Tejedor, F. Flores, and E. Louis, J. Phys. C **10**, 2163 (1977).